

Green's function elements obtained from Fireballs-96 (20). This is a pseudopotential density functional technique, implemented here with a minimal numerical basis for H, C, and S, and an sp^3d^5 basis for Au. The molecular structure was first optimized with Hellmann-Feynman forces, with the molecule embedded in an infinite octanedithiol matrix between two gold slabs. The two-dimensional unit cell consisted of an octanedithiol molecule connected at each end to a 2×2 Au surface. The terminal H was removed from each thiol group,

and the sulfur atoms were found to bind to the gold about 0.194 nm above the surface and equidistant from three Au surface atoms. The current was calculated for this geometric structure by contacting a single molecule between a pair of Au(111) clusters four by four by five atoms deep (avoiding technical problems for current calculations in an infinite system). A similar process was used for the nonbonded structure.

19. V. Mujica, M. Kemp, M. A. Ratner, *J. Chem. Phys.* **101**, 6849 (1994).

20. A. A. Demkov, J. Ortega, O. F. Sankey, M. P. Grumbach, *Phys. Rev.* **B52**, 1618 (1995).
 21. J. I. Siepmann, I. R. McDonald, *Phys. Rev. Lett.* **70**, 453 (1993).
 22. J. B. Schlenhoff, M. Li, H. Ly, *J. Am. Chem. Soc.* **117**, 12528 (1995).
 23. We thank L. Nagahara (Motorola Labs) and G. Ramachandran (Arizona State University) for useful discussions. Supported by NSF.

12 July 2001; accepted 27 August 2001

Present-Day Crustal Deformation in China Constrained by Global Positioning System Measurements

Qi Wang,¹ Pei-Zhen Zhang,^{2*} Jeffrey T. Freymueller,³
 Roger Bilham,⁴ Kristine M. Larson,⁵ Xi'an Lai,¹ Xinzhao You,¹
 Zhijun Niu,² Jianchun Wu,² Yanxin Li,⁶ Jingnan Liu,⁷
 Zhiqiang Yang,⁸ Qizhi Chen³

Global Positioning System (GPS) measurements in China indicate that crustal shortening accommodates most of India's penetration into Eurasia. Deformation within the Tibetan Plateau and its margins, the Himalaya, the Altyn Tagh, and the Qilian Shan, absorbs more than 90% of the relative motion between the Indian and Eurasian plates. Internal shortening of the Tibetan plateau itself accounts for more than one-third of the total convergence. However, the Tibetan plateau south of the Kunlun and Ganzi-Mani faults is moving eastward relative to both India and Eurasia. This movement is accommodated through rotation of material around the eastern Syntaxis. The North China and South China blocks, east of the Tibetan Plateau, move coherently east-southeastward at rates of 2 to 8 millimeters per year and 6 to 11 millimeters per year, respectively, with respect to the stable Eurasia.

Asia is a modern example of large-scale continental deformation (Fig. 1) and an ideal natural laboratory for its studies. Unfortunately, much of the region is remote, and thus the kinematics of Asia has been, until recently, poorly understood. Although much of its late Cenozoic deformation is explained by the collision and subsequent penetration of India into Eurasia (1), how Eurasia deforms in response to the collision is still subject to debate (2, 3), and a complete kinematic description of deformation over the entire re-

gion has not been available. Existing kinematic models (4, 5) rely on sparse data sets that can only describe the complex deformation of Eurasia on length scales of 200 km or larger, and lack data from critical regions. We present a synthesis of GPS velocities in China and its vicinity that provides new insights into the kinematics of Eurasia.

Much of the actively deforming part of Eurasia lies within China, including the Tibetan plateau, and parts of the Himalaya, Tian Shan, and Pamir mountain ranges (Fig. 1). Since the early 1990s, several regional GPS networks for active tectonic studies were established in China and neighboring regions (6–15). These networks were surveyed in campaign mode, usually at 1- to 2-year intervals. Each individual network was originally designed to address local problems, and it has been difficult to merge the data together, due to different data analysis strategies. We obtain a self-consistent velocity field by analyzing the original raw data from several different regional networks and merging them into a self-consistent solution.

We combined original data from GPS campaigns carried out between 1991 and

2001 by 10 Chinese and U.S. agencies or universities (16). The regional GPS data were combined with continuous tracking data from a well-distributed set of global International GPS Service (IGS) stations using the GIPSY software (17). For data observed between 1991 and 1995, we used a global solution strategy in which parameters associated with GPS satellite orbits were estimated together with all station coordinates (18). A projection operator was applied to the covariance matrix to remove the components of the covariance matrix that are purely due to reference frame uncertainty (19). For data observed after 1995, a regional solution strategy was adopted, using fixed orbits and satellite clocks provided by NASA's Jet Propulsion Laboratory (20). A subset of IGS stations was used in the regional solutions (21). Next, the daily free network solutions were each transformed into the ITRF97 (International Terrestrial Reference Frame, epoch 1997.0) by estimating a seven-parameter similarity transformation for each (22). We estimated the transformation for each day, on the basis of the common stations that are present both in ITRF97 and in the daily solution, and weighted each station by their respective uncertainties. The 1250 daily solutions were used as data to determine the station velocities and station coordinates at epoch 1995.0 by a standard weighted least-squares adjustment (23). The velocities in ITRF97 were then transformed into velocities in a Eurasia-fixed reference frame (24). The aggregate velocity solution of 354 stations (25) provides an image, to date, of present-day crustal deformation in Asia (Fig. 2). The velocity solutions in both ITRF97 and Eurasia-fixed frames are available at *Science's* Web site (26). Most velocity uncertainties, propagated by the errors of Eurasia rotation parameters, are in the range of 1 to 4 mm/year, except some stations with an observation interval shorter than 1.5 years. The mean uncertainties in northward velocities relative to Eurasia are 2.2 mm/year and 2.4 mm/year for eastward components.

Stations located on the northern Ganges plains, south of the Himalaya, show northward movement (N19°–22°E) at a rate of 36 to 38 mm/year with respect to stable Eurasia (27), consistent with some previous studies (5, 13, 28). Bangalore (station IISC) in southern India has a velocity of 35.9 ± 1.0 mm/year in the direction of $N26.9^\circ \pm 1.7^\circ$ E. The

¹Institute of Seismology, China Seismological Bureau, Wuhan 430071, China. ²Center for Crustal Movement Studies and Institute of Geology, China Seismological Bureau, Beijing 100029, China. ³Geophysical Institute, University of Alaska, Fairbanks, AK 99775, USA. ⁴Department of Geological Sciences and CIRES, University of Colorado, Boulder, CO 80309, USA. ⁵Department of Aerospace Engineering Sciences, University of Colorado, Boulder, CO 80309, USA. ⁶First Crustal Deformation Monitoring Center, China Seismological Bureau, Tianjin 300180, China. ⁷School of Geodesy and Geomatics, Wuhan University, Wuhan, 430071, China. ⁸Department of Surveying Engineering, Chang'an University, Xi'an 710064, China.

*To whom correspondence should be addressed. E-mail: peizhen@public3.bta.net.cn.

REPORTS

similar velocity between Bangalore and those in the northern Ganges plains indicates that there is no significant deformation within the Indian plate (28). The maximum velocity (~ 38 mm/year) of sites in the northern Ganges plains approximates the rate of convergence between the Indian and Eurasian plates. This total convergence rate is intermediate between that estimated in the NUVEL-1A model (~ 47 mm/year, $N24^\circ E$) (29, 30) and that reestimated recently on the basis of a revised plate configuration in the Indian ocean (~ 37 mm/year, $N38^\circ E$) (31). Our estimate is also similar to that (36 ± 3.5 mm/year, $N27.1^\circ E$) inferred from both Quaternary fault slip rates and GPS geodesy (5).

In the Tian Shan of northwest China (Fig. 1), widespread active faulting and folding, recent uplift, and high seismicity attest to rapid crustal shortening. Across its western part near Kashgar, velocities of 20 to 22 mm/year in the south decrease to ~ 0 in the same fashion as seen in Kirghizia, confirming the proposition that the total shortening rate across the western Tian Shan is ~ 20 mm/year (7). The total shortening rate between longitudes $81^\circ E$ and $85^\circ E$ is only 4.7 ± 1.5 mm/year. Eastward, the rate between longitudes 86° and 87°

decreases to < 1 mm/year, consistent with conclusion of eastward decreases of crustal shortening inferred from theoretical modeling and geological investigations (32, 33). A substantial amount of shortening must be accommodated to the north between the Tian Shan and Altai, as well as farther north in Mongolia.

The North China region includes the Ordos block and the North China Plain. The GPS measurements show coherent east-southeastward movement at rates of 2 to 8 mm/year to the direction of $N120^\circ - 140^\circ E$ [Fig. 2 and Supplementary fig. 1 (26)]. Major active faults in the North China region trend north-northeast ($N15^\circ - 25^\circ E$). The oblique intersections with the south-southeastward movement probably produce right-lateral strike-slip components along those faults, which cause major earthquakes with the same prominent component.

On the basis of 36 GPS stations distributed throughout the South China region [Fig. 2 and Supplementary fig. 2 (26)], we obtain an average velocity of 6 to 11 mm/year with respect to stable Eurasia oriented toward an azimuth of $N100^\circ - 130^\circ E$. These results are similar to Very Long Baseline Interferometry (VLBI) measurements (34) and previous

GPS measurements (using fewer stations) (13, 14). Because the 36 stations cover the entire South China block, we conclude that it behaves as a rigid block without internal deformation (1, 5, 6, 13, 14).

The Tibetan plateau undergoes substantial internal shortening (Fig. 3), with the direction of maximum shortening being $\sim N21^\circ E$, the inferred India-Eurasia convergence direction (27). Along a $N21^\circ E$ profile passing through the eastern part of the Tibetan plateau and Qilian Shan (Fig. 2), the ~ 38 mm/year convergence rate between the Indian plate and the rigid Alashan block north of the Qilian Shan represents more than 90% of the total collision rate between the Indian and Eurasian plates. The $N21^\circ E$ velocity gradient is strikingly linear except for a high-velocity gradient across the Himalaya at the southern margin of the plateau. The average convergence strain rate in this direction is $\sim 2 \times 10^{-8}$ year $^{-1}$. Taking ~ 16 mm/year for the convergence rate across the Himalaya, ~ 12 mm/year, or more than 30% of the total India-Eurasia convergence, is absorbed by internal shortening of the plateau (Fig. 3). An additional 10 mm/year of contraction occurs across the Qaidam basin and the Qilian Shan (Fig. 3).

This shortening must be broadly distrib-

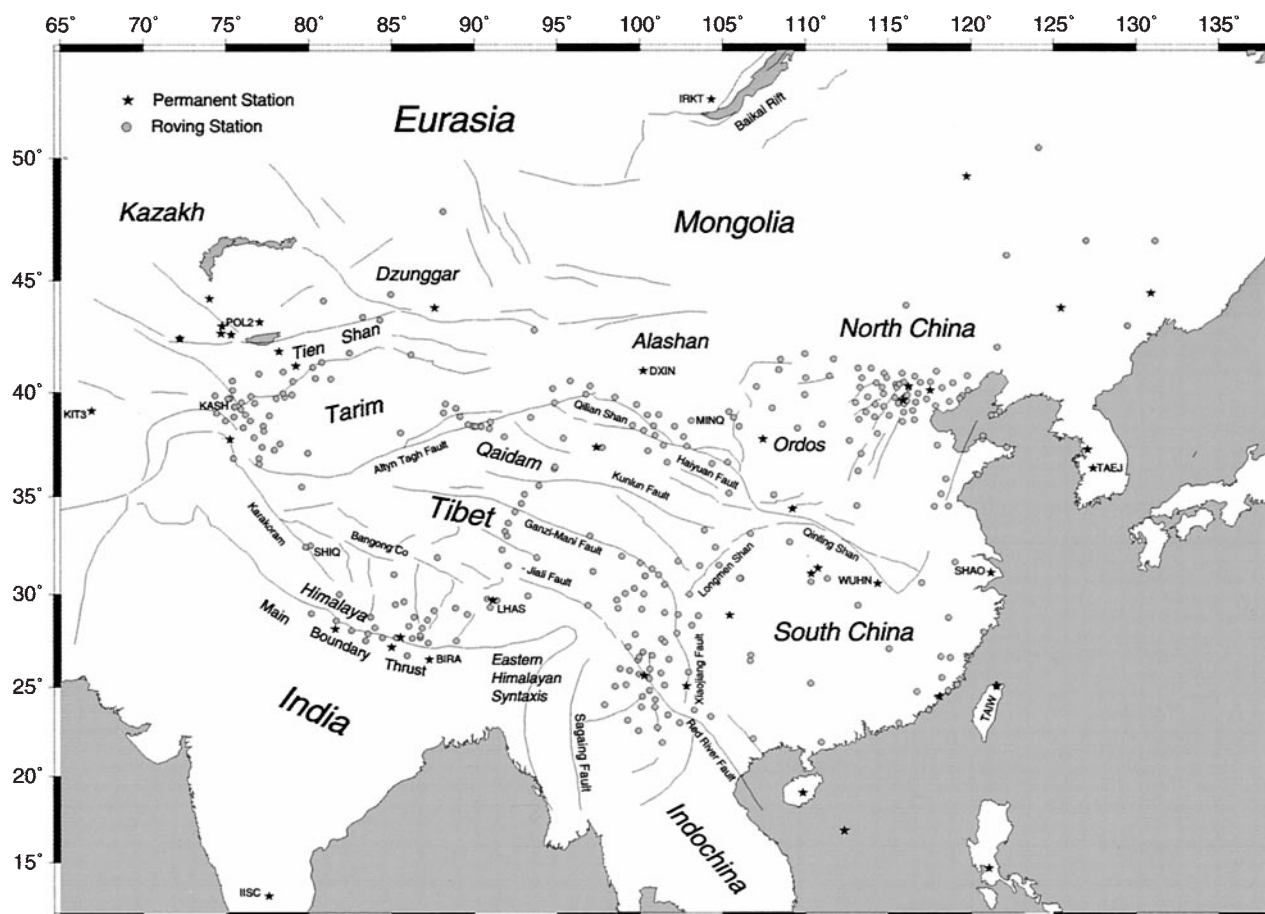


Fig. 1. Generalized map of active faults in China and vicinity showing the distribution of GPS stations used in this study. Black lines are major active faults. Circles represent roving GPS stations, and stars represent permanent GPS stations.

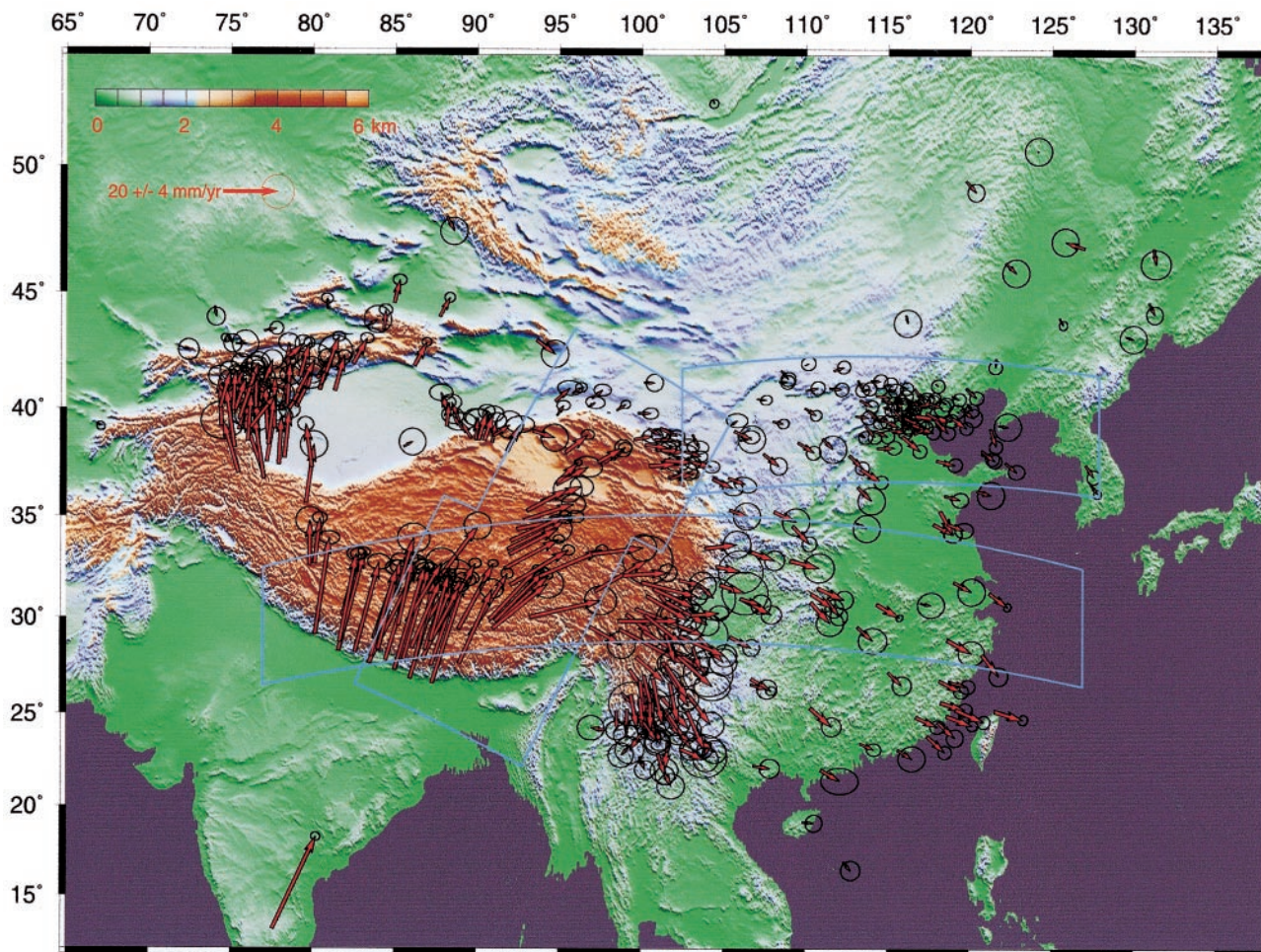


Fig. 2. GPS velocity vectors (mm/year) with respect to the stable Eurasia, plotted on a shaded relief map of the Asia topography (gtopo30). The ellipses denote the region of 1- σ error. The

polygons define three regions in which station velocities are used to formulate profiles shown in Fig. 3 and Supplementary figs. 1 and 2 (26).

uted; there would be a significant deviation from the linear trend if there were any single faults that took up a considerable fraction of this shortening. Thus, continuum rather than block-like deformation appears to characterize present-day tectonics of the Tibetan Plateau. This continuum deformation, however, seems to be limited to the plateau itself. Rigid block-like motion appears to characterize deformation of the regions to the north (the Tarim block), northeast (the Alashan and the Ordos block), and east (the South China block), and there are zones of concentrated contraction at both the north and south margins of the plateau (Figs. 2 and 3).

Although contraction appears to accommodate most of the convergence of India, the eastern Tibetan Plateau, south of the left-lateral Kunlun and/or Ganzi-Mani strike-slip faults, is moving eastward relative to both India and Eurasia (Figs. 1 through 3). The Tibetan plateau is not an undeformed wedge-shaped block extruding eastward (35), but instead, the eastern Tibetan Plateau is deforming internally, and

moving rapidly eastward. As noticed by Holt *et al.* (5), the N111°E component of velocities (orthogonal to the convergence direction) increases steadily northward from the Himalaya across the breadth of the Tibetan Plateau, then decreases rapidly as a result of left-lateral slip on the Ganzi-Mani and Kunlun faults, totaling about 12 to 14 mm/year (Fig. 3). If all of this left-lateral motion were on the Kunlun fault, these results would agree with the recent geological slip rate estimate for the Kunlun fault (36).

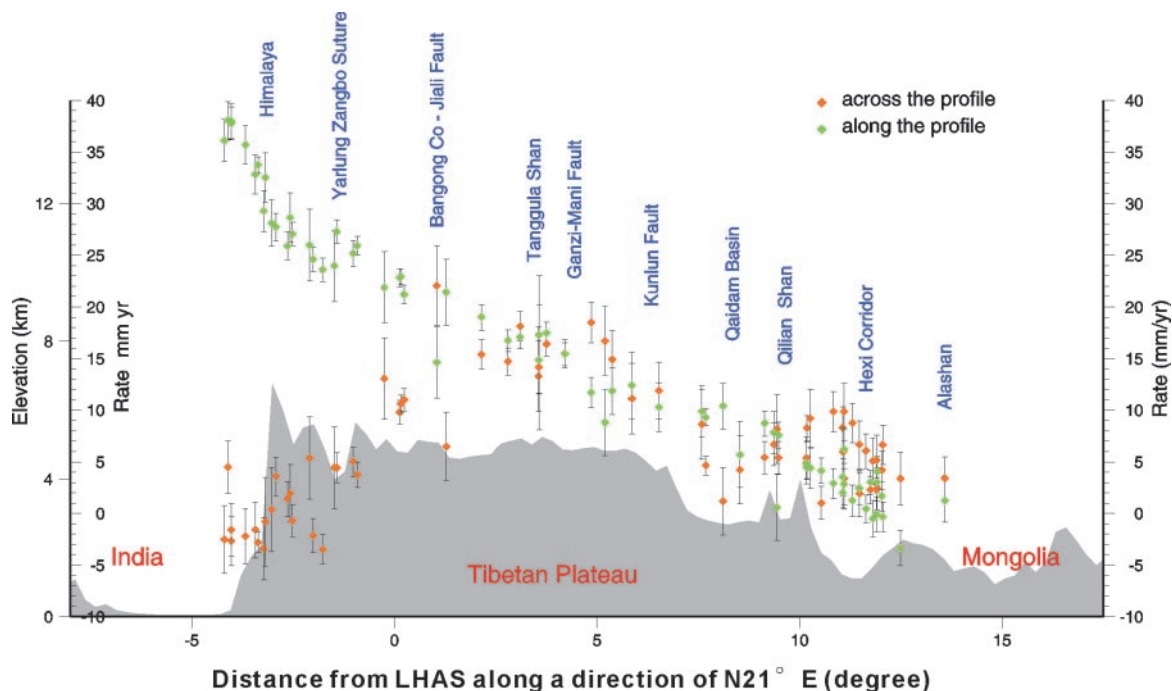
A series of north-trending normal faults and grabens characterized the eastward extension in the southern Tibet (37, 38). GPS measurements indicated that the rate of extension across southern Tibet between longitudes 80° and 90° is 20 ± 3 mm/year [Supplementary fig. 2 (26)], which is similar to the 18 ± 9 mm/year seismological rate (37).

Sites in the eastern Tibetan plateau show a prominent clockwise rotation. In the eastern margin of the Tibetan Plateau, stations move eastward in western Sichuan,

southeastward in northern Yun-nan, and south-southeastward in southern Yun-nan (Fig. 2). Together with stations in southern Tibet, the velocities show a clockwise rotation around the Eastern Himalayan Syntaxis (5, 9, 13).

The eastern part of the Tibetan Plateau moves eastward faster than does South China. Eastward station velocities in east-central Tibet are 21 to 26 mm/year, decreasing to 14 to 17 mm/year on the eastern margin of the Tibetan Plateau and 6 to 10 mm/year in the northern South China Block [Supplementary fig. 2 (26)]. Chen *et al.* (13) documented a lack of Cenozoic shortening across the Longmen Shan at the eastern boundary of the Tibetan plateau, and GPS results show a lack of present-day convergence as well (9, 13). If we simply assume that the velocity difference between eastern Tibet and South China results from convergence across the Longmen Shan, we would get a 5 to 11 mm/year crustal shortening rate across the Longmen Shan. This is larger than the results (<3 mm/year) of

Fig. 3. GPS velocity profile across the Tibetan Plateau in the direction of N21°E, parallel to the predicted direction of Indian-Eurasian collision. The red diamonds represent the N21°E component of velocity, which is parallel to the direction of the profile, and the green diamonds mark the N111°E component of velocity, which is perpendicular to the profile. The N21°E component shows a general linear trend of velocity gradient except for a high gradient across the Himalaya at the southern margin of the plateau. The N111°E component depicts eastward movement of the Central Tibetan Plateau with respect to both India and Mongolia.



Chen *et al.* (13), and would represent a serious conflict.

However, the clockwise rotation of the velocity vectors around the Eastern Himalayan Syntaxis suggests an alternate explanation, consistent with that proposed by King *et al.* (9) and Holt *et al.* (5). The extruding Tibetan crust rotates around the Eastern Himalayan Syntaxis, causing the southeastward to southward velocities observed in southern Yun-nan Province. Whether this clockwise rotation continues southwestward into Myanmar is unknown but entirely possible, because east-west contraction is suggested in western Myanmar, based on numerical kinematic models (4, 5). Thus, extruding Tibetan crust is neither overriding South China nor pushing it out over a free boundary in the South China Sea; it may be doing so to parts of Southeast Asia.

References and Notes

1. P. Molnar, P. Tapponnier, *Science* **189**, 419 (1975).
2. G. A. Houseman, P. England, *J. Geophys. Res.* **91**, 3651 (1986).
3. G. Peltzer, P. Tapponnier, *J. Geophys. Res.* **93**, 15095 (1988).
4. P. England, P. Molnar, *Geophys. J. Int.* **130**, 551 (1997).
5. W. E. Holt *et al.*, *J. Geophys. Res.* **105**, 19185 (2000).
6. W. Zhu *et al.*, *Sci. China D* **27**, 385 (1997).
7. K. Y. Abdрахmatov *et al.*, *Nature* **384**, 450 (1996).
8. R. Bilham *et al.*, *Nature* **336**, 61 (1997).
9. R. W. King *et al.*, *Geology* **25**, 179 (1997).
10. E. Calais *et al.*, *Geophys. Res. Lett.* **25**, 4003 (1998).
11. K. M. Larson *et al.*, *J. Geophys. Res.* **104**, 1077 (1999).
12. R. Bendick *et al.*, *Nature* **404**, 69 (2000).
13. Z. Chen *et al.*, *J. Geophys. Res.* **105**, 16215 (2000).
14. Z. Shen *et al.*, *J. Geophys. Res.* **105**, 5721 (2000).
15. Q. Wang *et al.*, *Sci. China D* **31**, 529 (2001).
16. China Seismological Bureau, Xi'an Institute of Surveying and Mapping, Chinese Academy of Science,

- Chinese National Bureau of Surveying and Mapping, University of Alaska, University of Colorado, Wuhan University, Chang'an University, Xinjiang Seismological Bureau, and Fujian Seismological Bureau.
17. S. M. Lichten, J. S. Border, *J. Geophys. Res.* **92**, 12751 (1987).
18. K. M. Larson, J. T. Freymueller, S. Philipson, *J. Geophys. Res.* **102**, 9961 (1997).
19. M. B. Heflin *et al.*, *Geophys. Res. Lett.* **19**, 131 (1992).
20. J. F. Zumberg *et al.*, *J. Geophys. Res.* **102**, 5005 (1997).
21. We used data, when available each day, from IGS stations in Eurasia, such as WUHN, KIT3, LHAS, IISC, TSKB, USUD, IRKT, BAH, ZWEN, KSTU, SELE, POL2, YAKZ, XIAN, KUNM, URUM, NTUS, BAKO, TAEJ, and SUWN. These stations are also used to transform daily solutions into the ITRF97.
22. P. Sillard, Z. Altamimi, C. Boucher, *Geophys. Res. Lett.* **25**, 3223 (1998).
23. Each daily solution includes at least one of the roving stations shown in Fig. 1. The numbers of annual daily solutions from 1991 to 2001 are 38, 29, 35, 57, 107, 97, 149, 153, 283, 126, and 176, respectively. Meanwhile, we include in our network adjustment weekly averaged estimates and covariances of globally distributed permanent stations, provided by Jet Propulsion Laboratory (SINEX files, GPS week 0814-1128 available at <http://cddis.gsfc.nasa.gov>) on the purpose of realization of Eurasia-fixed frame.
24. The Eurasia reframe is realized by subtracting the rotation of the Eurasian plate relative to the ITRF97 from GPS-derived station velocities. The Eurasian plate rotates at $0.2523 \pm 0.0035^\circ/\text{My}$ about a pole at $56.9 \pm 0.3^\circ\text{N}$, $-104.3 \pm 0.3^\circ\text{E}$ that is estimated by minimizing the adjustment to horizontal velocities of 11 stations within the stable Eurasia (ONSA, WZTR, NYAL, KOSG, METS, KIT3, KSTU, ZWEN, ARTU, POL2, and IRKT). The weighted rms of velocity adjustment for these 11 stations is 0.8 mm/year, to which POL2 and KSTU contribute most (1.6 and 2.4 mm/year, respectively). We tested other sets of stations to estimate the Eurasia motion. Different realizations of the Eurasia-fixed frame produce variations by no more than 2 to 3 mm/year in the southward components of all velocities, and much smaller differences in the eastward component.
25. We estimated a total of 432 station velocities, of

- which 78 were removed due to short time span (<1 year) or close location (<3 km) with other marks. Velocity tables including the remaining velocities in the Eurasia frame and ITRF97 are available at the Science Web site (26).
26. Supplementary material is available at www.sciencemag.org/cgi/content/full/294/5542/574/DC1.
27. We assume the average direction of motions of stations along the Lesser Himalaya represents the convergence direction between India and Eurasia. The motion of Indian plate relative to Eurasia is described about pole (27.3°N , 23.0°E , $0.40^\circ/\text{My}$), estimated from one station at Bangalore (IISC) and four stations along the Less Himalaya (MAHE, NEPA, BIRA, and JANK). Our study shows that the current velocity of India is ~22% slower than predicted by the NUVEL-1A model
28. J. Paul *et al.*, *Geophys. Res. Lett.* **28**, 647 (2001).
29. C. DeMets, R. G. Gordon, D. F. Argus, S. Stein, *Geophys. J. Int.* **101**, 425 (1990).
30. C. DeMets, R. G. Gordon, D. F. Argus, S. Stein, *Geophys. Res. Lett.* **21**, 2191 (1994).
31. R. G. Gordon, D. F. Argus, M. B. Heflin, *Eos* **80**, F273 (1999).
32. P. Zhang *et al.*, *Earthquake Res. China* **12**, 127 (1996).
33. J. P. Avouac, P. Tapponnier, *Geophys. Res. Lett.* **20**, 895 (1993).
34. P. Molnar, J. M. Gipson, *J. Geophys. Res.* **101**, 545 (1996).
35. R. Armijo, P. Tapponnier, T. Han, *J. Geophys. Res.* **94**, 2787 (1989).
36. J. V. Woerd *et al.*, *Geology* **26**, 695 (1998).
37. P. Molnar, Q. Deng, *J. Geophys. Res.* **89**, 6203 (1984).
38. R. Amijo *et al.*, *J. Geophys. Res.* **91**, 13803 (1986).
39. We thank P. Molnar for a thoughtful review of the preprint of the paper. We also thank Z. Shen at University of California Los Angeles and P. Fang at University of California San Diego for their help. The thoughtful reviews by two anonymous referees are greatly acknowledged. This work has been supported by National Key Basic Research Program (G19980407), National Science Foundation of China (49825104), National Major Scientific Infrastructure Program (CMONOC), and National Climbing Project to authors in China; and NSF grants to J.T.F. (EAR-9725563), R.B. (EAR-9306190), and K.M.L. (EAR-9727652) in the United States.

20 June 2001; accepted 19 September 2001